

RESEARCH PAPER



## Anticancer activity and toxicity of new quaternary ammonium geldanamycin derivative salts and their mixtures with potentiators

Natalia Skrzypczak<sup>a</sup>, Krystian Pyta<sup>a</sup>, Piotr Ruszkowski<sup>b</sup>, Przemysław Mikołajczak<sup>b</sup>, Małgorzata Kucińska<sup>c</sup>, Marek Murias<sup>c</sup>, Maria Gdaniec<sup>a</sup>, Franz Bartl<sup>d</sup> and Piotr Przybylski<sup>a</sup>

<sup>a</sup>Faculty of Chemistry, Adam Mickiewicz University, Poznan, Poland; <sup>b</sup>Department of Pharmacology, Poznan University of Medical Sciences, Poznan, Poland; <sup>c</sup>Department of Toxicology, Poznan University of Medical Sciences, Poznań, Poland; <sup>d</sup>Lebenswissenschaftliche Fakultät, Institut für Biologie, Biophysikalische Chemie Humboldt-Universität zu Berlin Invalidenstrasse 42, Berlin, Germany

### ABSTRACT

Geldanamycin (**GDM**) has been modified by different type neutral/acidic/basic substituents (**1–7**) and by quinuclidine motif (**8**), transformed into ammonium salts (**9–13**) at C(17). These compounds have been characterised by spectroscopic and x-ray methods. Derivative **8** shows better potency than **GDM** in MCF-7, MDA-MB-231, A549 and HeLa (IC<sub>50</sub>s = 0.09–1.06 μM). Transformation of **8** into salts **9–13** reduces toxicity (by 11-fold) at attractive potency, e.g. MCF-7 cell line (IC<sub>50</sub>~2 μM). Our studies show that higher water solubility contributes to lower toxicity of salts than **GDM** in healthy CCD39Lu and HDF cells. The use of **13** mixtures with potentiators PEI and DOX enhanced anticancer effects from IC<sub>50</sub>~2 μM to IC<sub>50</sub>~0.5 μM in SKBR-3, SKOV-3, and PC-3 cancer cells, relative to **13**. Docking studies showed that complexes between quinuclidine-bearing **8–13** and Hsp90 are stabilised by extra hydrophobic interactions between the C(17)-arms and K58 or Y61 of Hsp90.

### ARTICLE HISTORY

Received 15 June 2021  
Revised 19 July 2021  
Accepted 21 July 2021

### KEYWORDS

Ansamycins; benzoquinones; chaperone Hsp90; anticancer; SAR

### Introduction

Geldanamycin (**GDM**, Figure 1), a natural ansa-macrolide produced by *Streptomyces hygroscopicus*, has two unique structural features, namely a rigid benzoquinone ring and an aliphatic *ansa*-bridge that are linked together to form a characteristic basket-like structure.<sup>1</sup> Similar to other *ansa*-macrolides with benzene or benzoquinone core, it shows potent activity in different cancer cell lines.<sup>2–4</sup> Unfortunately, the significant toxicity of **GDM** impedes its future medical applications. This toxicity is believed to originate from 1,4-Michael conjugate addition/aromatisation/oxidation cascade with glutathione, yielding a C(19)-adduct.<sup>5–7</sup> In search for more active and less toxic benzoquinone and non-benzoquinone ansamycins as well as those with an expanded macrocyclic system, **GDM** was modified at the C(17), C(19) positions and at the methoxy, urethane or hydroxyl groups.<sup>2,8–10</sup> The most promising candidates among the C(17)-derivatives of **GDM** are amine derivatives 17-DMAG and 17-AAG that are currently under consideration or are in various phases of clinical trials.<sup>2,11–13</sup> Non-quinone analogues of **GDM** (reblastatin analogues, Bioteca, Cambridge, UK) or those containing halogens, saccharides, phenol groups at the core, were obtained by sequences of mutasynthetic, semi-synthetic, and total synthetic approaches. These analogues showed attractive activities against the cancer cell lines, such as human breast adenocarcinoma (SKBR-3, MCF-7, and MDA-MB-231), ovarian adenocarcinoma (SKOV-3), lung adenocarcinoma (A-549), and prostate adenocarcinoma (PC-3).<sup>2,4,14–20</sup> Moreover, modifications at the *ansa*-macrolide correlated to the preparation of conjugates with biotin, foliate, or within incorporated triazole bridge, that

gained molecular probe features of improved biocompatibility.<sup>21–24</sup> Overall, the *ansa*-bridge modifications of **GDM** led to a less effective anticancer potency than those performed at the rigid benzene or benzoquinone cores.<sup>25–33</sup> This can be attributed to a restriction of the *ansa*-bridge flexibility that is necessary for binding the **GDM** analogues to their molecular target, i.e. heat shock proteins Hsp90. Hsp90 shows an ATPase activity, which is required to fold proteins in cells in order to achieve their full functionality.<sup>2,34–36</sup> Crystal structures of **GDM** and 17-DMAG complexed with NBD of Hsp90 showed that the ligand conformation significantly differs from that of unbound molecule in solutions.<sup>27,28</sup> Interestingly, modifications of **GDM** at C(17) and C(19) positions sometimes resulted in antiviral potency against herpes (HSV), hepatitis B and C (HCV, HBV) or HIV-1.<sup>37–39</sup> Additionally, for **GDM** amine analogues where the C(17) substituent was bridged with the neighbouring quinone group at C(18), despite their good water solubility (e.g. guanidine-like derivatives), it was noticed that the bulkiness of the incorporated alkyl or aryl substituent was important for anticancer potency.<sup>40</sup> Ge et al. obtained reduced (hydroquinone) and highly water-soluble **GDM** derivatives with allylamine or *N,N*-dimethylethylamine in the form of salts that are considered in cancer therapy in phase I clinical trials.<sup>41</sup>

Recently, we have reported synthesis and anticancer activity of a series of C(17)-**GDM** derivatives and we found that rigidity of the C(17)-arm incorporating carbonyl group and lipophilicity are essential factors influencing an efficient binding of **GDM** analogues to Hsp90 and their anticancer potency.<sup>7</sup> Here, we report the anticancer activity studies of the **GDM** amine-quinuclidine analogue **8** with C(17)-arm of basic, rigid, and bulky nature. The

**CONTACT** Piotr Przybylski  [piotrp@amu.edu.pl](mailto:piotrp@amu.edu.pl)  Faculty of Chemistry, Adam Mickiewicz University, Uniwersytetu\_Poznanskiego 8, Poznan 61-614, Poland

 Supplemental data for this article can be accessed [here](#).

© 2021 The Author(s). Published by Informa UK Limited, trading as Taylor & Francis Group.

This is an Open Access article distributed under the terms of the Creative Commons Attribution License (<http://creativecommons.org/licenses/by/4.0/>), which permits unrestricted use, distribution, and reproduction in any medium, provided the original work is properly cited.

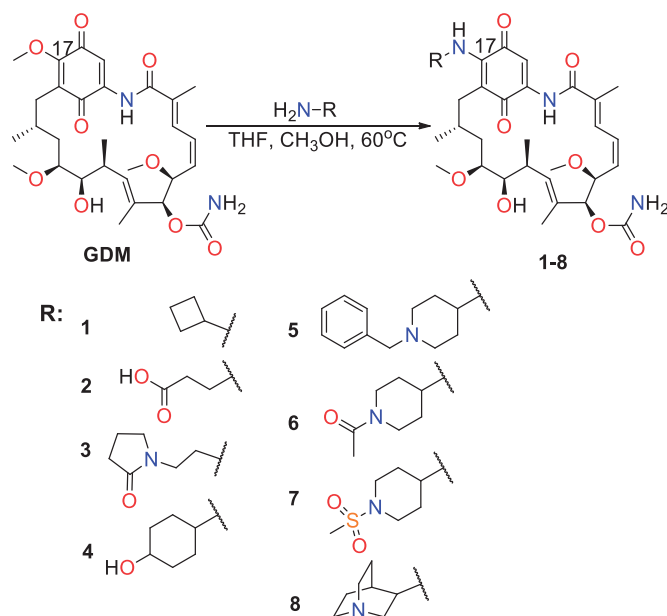


Figure 1. Geldanamycin (GDM) and its C(17)-analogues.

data have been determined for nine cancerous (MDA-MB-231, MCF-7, HeLa, HepG2, SKBR-3, SKOV-3, PC-3, U-87, and A-549) and two healthy (human lung fibroblasts CCD39Lu, human dermal fibroblasts HDF) cell lines. The activities of **8** are compared with the **GDM** derivatives **1–7** of acidic, basic, and neutral nature (Figure 1)<sup>7,23,40</sup>. Taking into account the fact that improved water solubility may lead to better bioavailability, derivative **8** was transformed into quaternary *N*-alkylammonium salts **9–13** of different *N*-tail structure (Figure 2). Moreover, **GDM** quinuclidine salts were also studied in mixtures with potentiators towards their anticancer potency and in order to obtain information about their toxicity.

## Results and discussion

### Synthesis of GDM analogues

**GDM** derivatives **1–8** were obtained according to the earlier reported protocol<sup>7</sup> and their structures were confirmed by <sup>1</sup>H, <sup>13</sup>C NMR, and 2D NMR, FT-IR, and ESI MS methods (Supplementary Material). Derivatives **1–3** formed single crystals that allowed to determine their structures by X-ray analysis (Table 1S, Figures 53S–59S, Supplementary Material). Comparison of the <sup>1</sup>H and <sup>13</sup>C NMR spectra of **8** and its *N*-alkylammonium salts (**9–13**) with those of **1–7** showed only minor differences in the position of the proton and the carbon atom resonances assigned to the quinone and the *ansa*-bridge parts (Figure 60S; Supplementary Material). The NOESY contacts for **GDM** analogues indicated *trans*-configuration of the lactam group with the lactam proton directed into the macrocyclic cavity, as shown in Figure 60S. As found for **8** and **9–13** salts, the absolute value of the H(29)–C(29)–N(17)–H(17) torsion angle is in the range of 120–130° (<sup>3</sup>J<sub>N(17)H-H(29)</sub>~6.5–8 Hz), and the *N*-alkyl substituent of nitrogen *N* + (30) is oriented away from the quinone core (Figure 60S). The nitrogen atom N(17), linking the **GDM** and quinuclidine parts, seems to be present in a distorted *sp*<sup>2</sup> hybridisation, as suggested by DFT calculations (Figure 60S). The above data indicated similar conformations of **GDM** derivatives in its “free form” in solution and solid, with only small changes in orientation of the C(17)-amine part relative to the quinone core.

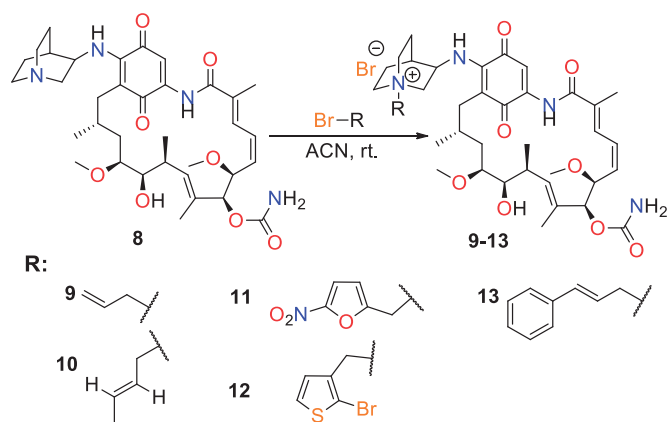


Figure 2. Quaternisation of the quinuclidine *N* atom within **8** leading to analogues **9–13**.

### Anticancer potency and toxicity in normal cells of GDM analogues

Quinuclidine derivative **8** and its quaternary *N*-alkylammonium salts (**9–13**) were initially tested in MDA-MB-231, MCF-7, HeLa, and HepG2 and healthy CCD39LU cell lines, and compared with biological test results of typical **GDM** C(17)-derivatives (**1–7**) (Table 1). Although **GDM** belongs to the known and active anticancer agents, its potency against breast cancer cells (MCF-7) is the lowest among the studied analogues (Table 1, IC<sub>50</sub> = 3.51 μM). A comparison of **GDM** activity and its analogues in the MCF-7 indicates that derivatives **1**, **3**, and **8** are markedly more potent than **GDM**, which is reflected by their low IC<sub>50</sub>~0.1 μM values. Furthermore, **1**, **3**, and **8** show higher SI indexes (~77, 75, and 10) than **GDM** for the MCF-7 cell line. Derivatives **5–7** were also more potent than **GDM** in the MCF-7 cell line (IC<sub>50</sub>~1 μM), with still favourable SIs~10. Lipophilicity of the most promising analogues (**1**, **3**, and **5–8**) is relatively good (clog*P* = 0.7–3.4) and comparable with that of **GDM** (clog*P*~2). Compound **2**, bearing a terminal acidic group, showed the lowest activity in the MCF-7 cell line at a less favourable SI compared to **GDM**. Taking into account the binding models of **GDM** and its derivatives with Hsp90, one should expect that the carboxylic group might improve the binding strength as a result of the interaction with a positively charged K58<sup>7,27,28</sup>. However, it is likely that in solution a flexible C(17) arm of **2** takes part in competitive intramolecular interactions (see Supplementary Material, Figure 51S), preventing the expected stabilising interaction with K58 of Hsp90. The existence of the H-bonded structures of **2** in solution and its relatively low lipophilicity (clog*P*~0.4, Table 1), might explain the lower anticancer activity of **2** compared to the analogues **1**, **3**, and **8**. In addition to low anticancer potency, compound **2** exhibits also very low toxicity when compared with **GDM** (IC<sub>50</sub> (CCD39Lu) = 20.8 μM, Table 1). As for other biological data for **1–8**, the quinuclidine analogue **8** shows the most beneficial potency in MDA-MB-231 (IC<sub>50</sub> = 0.14 μM) among all ansamycins studied. The activity of **8** relative to **GDM** was improved, not only in MDA-MB-231 but also in other studied cancer cell lines (Table 1). When compared with **8**, **GDM** was only more active in HepG2 cells. Lower activity than that of **GDM** was also observed for all other studied derivatives (**1–7**) and salts (**9–13**) in the HepG2 cancer cell line. The most promising quinuclidine analogue **8** exhibited relatively high toxicity in healthy cells CCD39Lu (IC<sub>50</sub> = 0.87 μM) and had only low SI indexes (SIs < 1, Table 1).

Considering the above results, we decided to further test compound **8** using the 2nd panel of cancer cell lines: SKBR-3, SKOV-3,

**Table 1.** The IC<sub>50</sub> values [(μM) ± SD], selectivity indexes [SI<sub>CCD39Lu</sub>] as well as clogP and solubility S<sub>H<sub>2</sub>O</sub> parameters for **GDM** and its analogues 1–8 and salts (9–13) obtained in MDA-MB-231, MCF-7, HeLa, HepG2, and CCD39Lu (1st panel) cell lines.

Cmpd.	MDA-MB-231	MCF-7	HeLa	HepG2	CCD39Lu	clogP	Solubility S <sub>H<sub>2</sub>O</sub> (mg/mL)
<b>GDM</b>	1.04 ± 0.63 [SI 8.17]	3.51 ± 0.21 [SI 2.42]	1.42 ± 0.10 [SI 5.99]	0.74 ± 0.32 [SI 11.48]	8.50 ± 0.25	0.43/ 2.15*	–
<b>1</b>	2.45 ± 0.78 [SI > 4.08]	0.13 ± 0.01 [SI > 76.92]	1.67 ± 0.54 [SI > 5.99]	1.75 ± 0.04 [SI > 5.71]	>10	2.24	–
<b>2</b>	4.27 ± 1.54 [SI 4.87]	7.62 ± 2.35 [SI 2.73]	3.48 ± 0.51 [SI 5.98]	3.04 ± 0.47 [SI 6.84]	20.80 ± 5.14	0.43	1.47
<b>3</b>	1.84 ± 0.33 [SI 4.08]	0.10 ± 0.21 [SI 75.00]	1.25 ± 0.22 [SI 6.00]	1.31 ± 0.54 [SI 5.73]	7.50 ± 0.55	0.67	0.05
<b>4</b>	>10 [SI > 1]	>10 [SI > 1]	>10 [SI > 1]	>10 [SI > 1]	>10	1.87	0.04
<b>5</b>	2.28 ± 0.54 [SI 6.71]	1.84 ± 0.57 [SI 8.32]	1.56 ± 0.14 [SI 9.81]	1.63 ± 0.49 [SI 9.39]	15.30 ± 0.12	3.40	–
<b>6</b>	3.16 ± 0.89 [SI > 3.16]	0.61 ± 0.14 [SI > 16.39]	4.75 ± 0.35 [SI > 2.11]	3.38 ± 0.13 [SI > 2.96]	>10	1.36	–
<b>7</b>	2.36 ± 0.35 [SI 5.34]	0.96 ± 0.51 [SI 13.13]	1.61 ± 0.61 [SI 7.83]	1.68 ± 0.32 [SI 7.50]	12.60 ± 0.21	1.38	–
<b>8</b>	0.14 ± 0.01 [SI 6.21]	0.09 ± 0.01 [SI 9.67]	1.06 ± 0.26 [SI 0.82]	1.25 ± 0.22 [SI 0.70]	0.87 ± 0.22	2.23	0.15
<b>9</b>	4.65 ± 2.65 [SI > 2.15]	2.34 ± 0.56 [SI > 4.27]	9.25 ± 0.98 [SI > 1.08]	>10 [SI > 1]	>10	–1.10	11.9
<b>10</b>	4.64 ± 1.51 [SI > 2.16]	2.51 ± 1.03 [SI > 3.98]	7.43 ± 3.21 [SI > 1.35]	>10 [SI > 1]	>10	–0.85	8.09
<b>11</b>	3.93 ± 1.60 [SI > 2.54]	4.67 ± 2.00 [SI > 2.14]	8.91 ± 3.19 [SI > 1.12]	8.86 ± 0.17 [SI > 1.13]	>10	–0.81	2.30
<b>12</b>	5.01 ± 2.15 [SI > 2.00]	2.65 ± 1.09 [SI > 3.77]	9.12 ± 1.81 [SI > 1.10]	>10 [SI > 1]	>10	0.37	4.50
<b>13</b>	4.66 ± 2.49 [SI > 2.15]	2.31 ± 0.97 [SI > 4.33]	8.14 ± 0.64 [SI > 1.23]	>10 [SI > 1]	>10	0.61	5.03

clogP calculated by Molinspiration<sup>42</sup>.

Selectivity index [SI<sub>HDF</sub>] = IC<sub>50</sub> normal cell line CCD39Lu/IC<sub>50</sub> respective cancer cell line.

**GDM**: geldanamycin.

PC-3, U-87, and A-549 and healthy cells HDF and to compare biological data with those of exemplary derivative **1** (Table 2). Our studies demonstrated that **8** is very active in the 2nd panel of cancer cell lines and its activity is even slightly better than that of **GDM** in the A-549 cell line (IC<sub>50</sub> = 0.99 μM). The potency of **8** in SKBR-3, SKOV-3, PC-3, and U-87 cancer cell lines was lower or comparable to **GDM** (Table 2). In contrast with the results obtained in normal CCD39LU cell line, the toxicity of **8** in healthy cells HDF, is significantly lower than that for **GDM** (Table 2). The potency of low-cytotoxic **1** (IC<sub>50(HDF)</sub> = 30 μM; IC<sub>50(CCD39Lu)</sub> = > 10 μM), especially in the 2nd panel of SKBR-3, SKOV-3, PC-3, U-87, and A-549 cancer cell lines, was relatively low (IC<sub>50</sub> ~ 7.5 μM). Taking into regard the fact that another analogue of low cytotoxicity, **2** (IC<sub>50(CCD39Lu)</sub> = 20.8 μM), shows the best water solubility among **1–8** derivatives (Table 1), we decided to transform the most active quinuclidine analogue **8** into its better water-soluble *N*-alkylammonium salts to investigate the influence of a polar structure of this type on anticancer activity vs. toxicity. Biological tests of the salts **9–13** in the 1st panel of cancer cell lines (Table 1) revealed that similar to **8**, they were generally more active than **GDM** in the MCF-7 cells (except **11**, Table 1). A comparison of IC<sub>50</sub> values between **8** and **9–13**, indicated higher activity of the former. Interestingly, the transformation of **8** into its salts **9–13** was beneficial regarding low toxicities of **9–12** in normal cell line CCD39Lu (Table 1). Among quaternary salts, analogue **13** with a bulky *N*-cinnamyl quinuclidine moiety showed the best activity in MCF-7 with IC<sub>50</sub> = 2.31 μM and with twice the value of SI index (SI = 4.33) when compared to **GDM**. Very good results in MCF-7 cells were also obtained for salts **9** (IC<sub>50</sub> = 2.34 μM) and **10** (IC<sub>50</sub> = 2.51 μM), which, like **13**, had no heteroatoms in the tail attached to the quinuclidine unit (Table 1). Other biological data for the 1st panel of cell lines showed that quaternisation of

**Table 2.** Anticancer activities [IC<sub>50</sub> (μM) ± SD] of **GDM** and its **1** and **8** analogues and salts (9–13) in SKBR-3, SKOV-3, PC-3, U-87, A-549 cells (2nd panel), and toxicity in human dermal fibroblasts (HDF) cell line [IC<sub>50</sub> (μM) ± SD] together with selectivity indexes [SI<sub>HDF</sub>].

Cmpd.	SKBR-3	SKOV-3	PC-3	U-87	A-549	HDF
<b>GDM</b>	0.87 ± 0.17 [SI 2.45]	0.94 ± 0.09 [SI 2.27]	0.73 ± 0.01 [SI 2.92]	0.81 ± 0.12 [SI 2.62]	0.99 ± 0.01 [SI 2.15]	2.13 ± 0.11
<b>1</b>	7.44 ± 0.09 [SI 4.03]	8.04 ± 0.24 [SI 3.73]	7.02 ± 0.06 [SI 4.28]	7.32 ± 0.49 [SI 4.10]	9.01 ± 0.63 [SI 3.33]	30.02 ± 1.03
<b>8</b>	1.49 ± 0.29 [SI 2.16]	1.16 ± 0.92 [SI 2.78]	1.47 ± 0.31 [SI 2.19]	1.08 ± 0.16 [SI 3.43]	0.94 ± 0.03 [SI 3.43]	3.22 ± 0.18
<b>9</b>	3.12 ± 0.01 [SI 1.70]	3.86 ± 0.05 [SI 1.37]	3.01 ± 0.11 [SI 1.76]	3.69 ± 0.08 [SI 1.43]	3.09 ± 0.01 [SI 1.71]	5.29 ± 0.17
<b>10</b>	1.94 ± 0.52 [SI 1.53]	1.61 ± 0.13 [SI 1.84]	1.88 ± 0.02 [SI 1.57]	1.84 ± 0.11 [SI 1.61]	1.29 ± 0.07 [SI 2.29]	2.96 ± 0.36
<b>11</b>	6.49 ± 0.07 [SI 1.22]	6.04 ± 0.38 [SI 1.31]	6.22 ± 0.13 [SI 1.27]	6.06 ± 0.58 [SI 1.31]	6.83 ± 0.32 [SI 1.16]	7.91 ± 0.91
<b>12</b>	8.49 ± 0.36 [SI 1.64]	8.02 ± 0.17 [SI 1.73]	7.94 ± 0.03 [SI 1.75]	8.58 ± 0.19 [SI 1.62]	8.94 ± 0.27 [SI 1.56]	13.91 ± 0.42
<b>13</b>	2.02 ± 0.11 [SI 1.89]	2.17 ± 0.06 [SI 1.76]	2.05 ± 0.09 [SI 1.86]	2.26 ± 0.15 [SI 1.67]	2.06 ± 0.01 [SI 1.85]	3.81 ± 0.11

Selectivity index [SI<sub>HDF</sub>] = IC<sub>50</sub> normal cell line HDF/IC<sub>50</sub> respective cancer cell line.

quinuclidine nitrogen in **8** significantly decreased potency in MDA-MB-231, HeLa and HepG2 cancer cell lines while toxicity was reduced in normal CCD39Lu cells (Table 1). Anticancer studies of salts **9–13** in the 2nd panel of cell lines (Table 2) revealed that the most active analogue is compound **10** with no heteroatoms in the *N*-quinuclidine tail. Its IC<sub>50</sub> values were oscillating around 1.7 μM (1.29 – 1.94 μM). The highest potency of **10** was registered in the A-549 cancer cell line (IC<sub>50</sub> = 1.29 μM). Although a comparison of anticancer activities of **GDM**, **8** and **10** (Table 2) showed the lowest potency for **10**, its activity remains attractive in the 2nd panel of cancer cells, at lower cytotoxicity than that of **GDM**



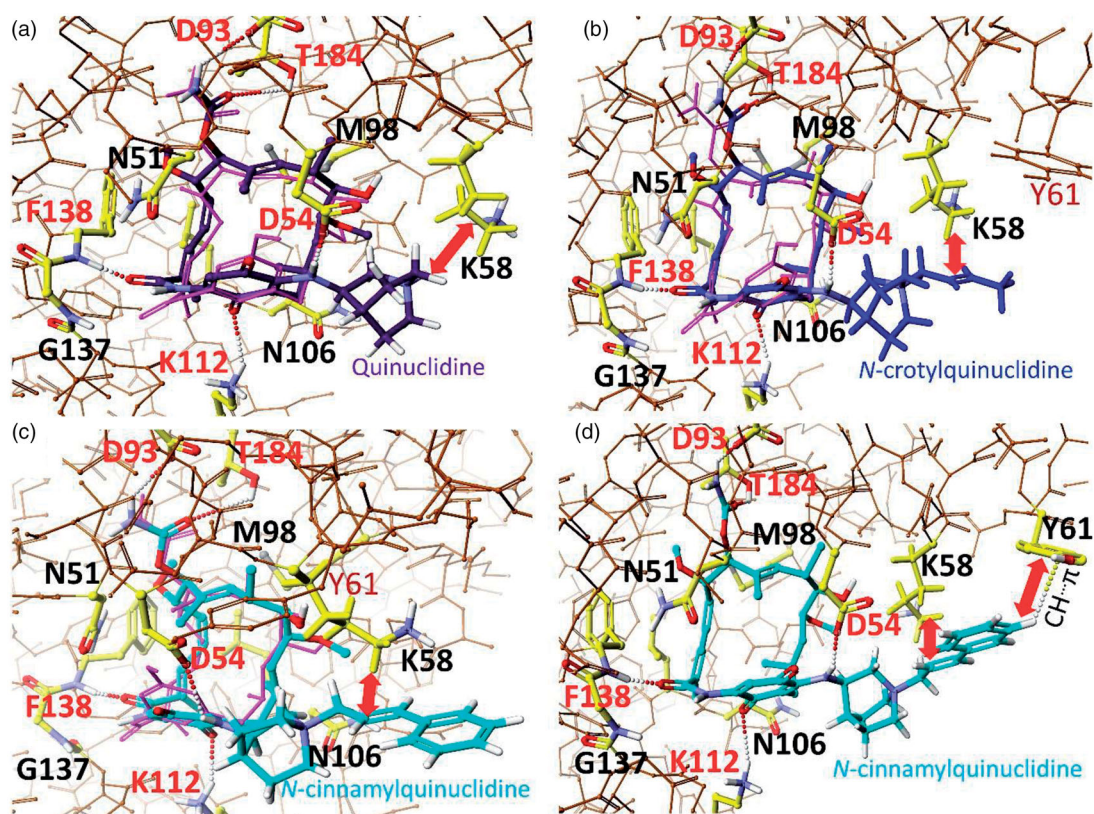


**Figure 3.** Binding models revealing interactions between *N*-binding domain (NBD) of Hsp90 (PDB 3Q5J[43]) and new ansamycin derivatives: **8** ( $\Delta H^{\circ}_f = -47$  kcal/mol/ (a), **10** ( $\Delta H^{\circ}_f = -39$  kcal/mol/ (b) and **13** in binding mode I ( $\Delta H^{\circ}_f = -32$  kcal/mol/ (c), and **13** in binding mode II ( $\Delta H^{\circ}_f = -37$  kcal/mol/ (d), compared to binding mode of macbecin II (PDB2VW5<sup>35</sup>, pink), and optimised by MOG-PM6 method (Scigress F.J. 2.6, EU 3.1.9);<sup>46</sup> amino acids of Hsp90 ATP-binding pocket are marked by yellow; intermolecular interactions (H-bonds) are marked by dots.

in HDF and CCD39Lu cell lines. Salts **9** and **13**, with substituents of similar nature as **10**, also showed good anticancer activities with  $IC_{50} \sim 2\text{--}3 \mu\text{M}$  and with a markedly reduced toxicity in HDF ( $IC_{50} \sim 5.29$  and  $3.81 \mu\text{M}$ , Table 2). To conclude, considering the biological results for **9**–**13** obtained in the 1st and the 2nd panel of cancer cell lines, when compared to the activity data of **GDM** and **8**, the most promising among the reported salts is salt **13** as it shows the best balance between the anticancer potency and toxicity in normal cells. It is relatively low toxic in both normal cell lines HDF ( $IC_{50} = 3.81 \mu\text{M}$ ) and CCD39LU ( $IC_{50} > 10 \mu\text{M}$ ) at still attractive level of anticancer potency  $IC_{50} \sim 2 \mu\text{M}$  in MCF-7, SKBR-3, SKOV-3, PC-3, U-87, and A-549 cell lines.

#### Binding mode of quinuclidine analogues of GDM and 9–13 salts with Hsp90

According to the earlier reports,<sup>7,26–28,32,43</sup> we assumed that docking of **8**, **10**, and **13** into the target, i.e. ATP-binding pocket of Hsp90, requires *trans/cis* isomerisation of the lactam group and drastic conformational changes within the *ansa*-bridge owing to atropisomerisation process, i.e. flipping of the *ansa*-bridge from one side of the benzoquinone ring to the other (Figure 62S, Supplemental Material). DFT calculated energy barrier is 36.97 kcal/mol for the total atropisomerisation process of **10** requiring *trans-cis* lactam isomerisation crucial for binding with NBD of Hsp90 (Figures 3(b) and Figure 62S; Supplemental Material). This value is higher than that estimated from earlier studies of **GDM** ( $E = 16\text{--}21$  kcal/mol).<sup>44,45</sup> Structural comparison between complexes of Hsp90 with **GDM** and **8**, showed that the mutual arrangements of the *ansa*-bridges and quinone cores

relative to the Hsp90 key amino acids are similar in both cases.<sup>7,27</sup> Atropisomerisation of active **GDM** analogues from the *trans*-lactam form (dominating in solution) into the *cis*-lactam one (bound with Hsp90) is evoked by the mutual induced fitting of human Hsp90 and the **GDM** derivative. The **8**-Hsp90 complex is stabilised by the formation of intermolecular H-bonds between the ansamycin and F138, D54, D93, K112, and T184 of Hsp90, whereas, e.g. M98 and K58 are involved in hydrophobic interactions of the ligand and in the ATP-binding pocket (Figure 3). Thus, the above binding mode of **8** is slightly improved relative to that known for **GDM** by an extra hydrophobic stabilisation of quinuclidine basket of **8** with K58, contributing also to improved anticancer potency of **8** relative to **GDM**. Comparison between calculated binding models of the most active derivative **8** and salts **10** and **13** of decreased cytotoxicity shows for the latter ones also possibility of hydrophobic stabilisation with K58 of Hsp90 (Figure 3). Comparison of binding energies of **10** ( $\Delta H^{\circ}_{f(10)} = -39$  kcal/mol) or **8** ( $\Delta H^{\circ}_{f(8)} = -47$  kcal/mol) with Hsp90 indicates the privileged formation of **8**-Hsp90 complex. This result is in line with higher anticancer potency of higher lipophilic **8** ( $\text{clog}P = 2.23$ ;  $S_{H_2O} = 0.15$  mg/mL, Table 1) when compared to better water-soluble **10** ( $\text{clog}P = -0.85$ ;  $S_{H_2O} = 8.09$  mg/mL, Table 1). Compound **13**, owing to the presence of its lengthy and bulky quinuclidine arm at C(17), has two alternative binding modes to Hsp90 (Figure 3(c,d)). The binding mode I of **13**, is analogous to that of **8** and **10** (the interaction with K58, Figure 3(c)). The binding mode II of **13** to Hsp90 is realised via a conformational change within the quinuclidine basket, where the *N*<sup>+</sup>-cinnamyl tail is involved in an intermolecular C-H $\cdots$  $\pi$  interaction with Y61 of Hsp90 (Figure 3(d)). A more favourable binding mode II to Hsp90 is excluded for **8** and **10** due to shorter quinuclidine arms at C(17). Overall, the higher anticancer

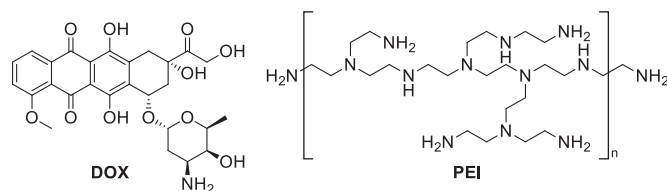


**Figure 4.** Structures of tested selected potentiators of quinuclidine analogues of **GDM**.

activity of **8** compared to **10** and **13** can be explained by a higher energetic profit of binding **8** to Hsp90 ( $\Delta H^{\circ}_f = -47$  kcal/mol) than for **10** ( $\Delta H^{\circ}_f = -39$  kcal/mol) and **13** ( $\Delta H^{\circ}_f = -37$  kcal/mol). Changes in lipophilicity (*clogP*) do not explain the differences in the anticancer effect of the tested salts (**9–13**). In turn, the better water solubility of salts **9**, **10**, and **13** ( $S_{H_2O} > 5$  mg/mL) seems to be in line with their better anticancer effects than **11** ( $S_{H_2O} = 2.30$  mg/mL) and **12** ( $S_{H_2O} = 4.5$  mg/mL), especially in the 2nd panel of tested cancer cell lines.

#### Anticancer tests of the most active quinuclidine analogues with potentiators

It is known that the effectiveness and potency of various antibiotics can be improved when they are used in cocktails with adjuvants and potentiators allowing, e.g. effective transportation of a drug into the target site of action.<sup>47–49</sup> In order to evaluate the influence of the addition of doxorubicin (**DOX**; **Figure 4**) or branched polyethylenediamine – (**PEI**, polyethylenimine; **Figure 4**) on the activity of our lead compounds **8** and **13**, tests were performed in SKBR-3, PC-3, SKOV-3, and HDF cells for their 1:1 equimolar mixtures (**Table 3**).

As shown in **Table 3**, **DOX** reveals a comparable activity at  $IC_{50} \sim 0.7$   $\mu$ M towards all studied cancer cell lines at enhanced toxicity in the HDF normal cell line, relative to those of **GDM** (**Table 2**). Compounds **8** and **13** are of lower potency in studied cancer cell lines, although they simultaneously exhibit reduced toxic effects in HDF cell line, when referred to **DOX** and **PEI**. With the addition of **PEI** to **8** and **13** opposite changes in the potency were noted. The equimolar mixture **13 + PEI** showed significantly improved potency relative to that of **13** ( $IC_{50(13+PEI)} \sim 0.6$   $\mu$ M vs.  $IC_{50(13)} \sim 2$   $\mu$ M). Interestingly **13 + PEI** mixture showed even slightly higher anticancer potency ( $IC_{50} = 0.62$   $\mu$ M) than **PEI** itself in SKOV-3 cells. Unfortunately, with the increased potency of mixture **13 + PEI**, its toxicity also showed a 3-fold increase in HDF cells in comparison with **13**. In turn, the combined use of **8** with **PEI** resulted in decreased anticancer activity and cytotoxicity, both relative to **8** and **PEI**. The use of **8+DOX** and **13+DOX** mixtures improved potency in SKBR-3 cells relative to **8** and **13**, respectively. For the **13+DOX** mixture, the analogous result was also obtained in SKOV-3 and PC-3, in contrast to **8+DOX**. The markedly enhanced anticancer activities of **13+DOX** in studied cancer cell lines relative to that of **13**, is accompanied by nearly preserved toxicity in HDF cells ( $IC_{50}$  level  $\sim 3$   $\mu$ M). Thus, our studies showed that the use of better water-soluble salt **13** than compound **8**, in an equimolar mixture with **PEI** and **DOX**, contribute to markedly improved anticancer activity in SKBR-3, SKOV-3, and PC-3 ( $IC_{50} \sim 3$   $\mu$ M), however, at the expense of increased toxicity in normal cells, when referred to **13**. Furthermore, tests with **13+DOX** mixture showed some available compromise between relatively preserved cytotoxicity (at the level  $IC_{50} \sim 3$   $\mu$ M) and enhanced anticancer potency to  $IC_{50} \sim 1$   $\mu$ M, especially in the PC-3 cell line ( $SI \sim 3$ ).

**Table 3.** Anticancer activities [ $IC_{50}$  ( $\mu$ M)  $\pm$  SD] of **8** and **13** and their equimolar 1:1 mixtures with **DOX** and **PEI** in SKBR-3, SKOV-3, and PC-3, compared with toxicity determined in normal human dermal fibroblasts (HDF) cell line [ $IC_{50}$  ( $\mu$ M)  $\pm$  SD] and selectivity indexes [ $SI_{HDF}$ ].

Cmpd.	SKBR-3	SKOV-3	PC-3	HDF
<b>8</b>	1.49 $\pm$ 0.29 [SI 2.16]	1.16 $\pm$ 0.92 [SI 2.78]	1.47 $\pm$ 0.31 [SI 2.19]	3.22 $\pm$ 0.18
<b>8 + DOX</b>	1.06 $\pm$ 0.08 [SI 2.42]	1.74 $\pm$ 0.02 [SI 1.48]	1.71 $\pm$ 0.11 [SI 1.50]	2.57 $\pm$ 0.07
<b>8 + PEI</b>	2.61 $\pm$ 0.11 [SI 1.53]	2.04 $\pm$ 0.01 [SI 1.96]	2.68 $\pm$ 0.03 [SI 1.49]	3.99 $\pm$ 0.22
<b>13</b>	2.02 $\pm$ 0.11 [SI 1.89]	2.17 $\pm$ 0.06 [SI 1.76]	2.05 $\pm$ 0.09 [SI 1.86]	3.81 $\pm$ 0.11
<b>13 + DOX</b>	1.33 $\pm$ 0.21 [SI 2.40]	1.49 $\pm$ 0.16 [SI 2.14]	1.09 $\pm$ 0.01 [SI 2.93]	3.19 $\pm$ 0.31
<b>13 + PEI</b>	0.55 $\pm$ 0.02 [SI 1.93]	0.62 $\pm$ 0.05 [SI 1.71]	0.59 $\pm$ 0.01 [SI 1.80]	1.06 $\pm$ 0.06
<b>DOX</b>	0.72 $\pm$ 0.04 [SI 2.11]	0.74 $\pm$ 0.06 [SI 2.05]	0.68 $\pm$ 0.01 [SI 2.24]	1.52 $\pm$ 0.03
<b>PEI</b>	0.53 $\pm$ 0.05 [SI 1.55]	0.69 $\pm$ 0.01 [SI 1.19]	0.51 $\pm$ 0.02 [SI 1.61]	0.82 $\pm$ 0.11

Selectivity index [ $SI_{HDF}$ ] =  $IC_{50}$  normal cell line HDF/ $IC_{50}$  respective cancer cell line.

#### Conclusions

The quinuclidine analogue **8** of **GDM** and its *N*-alkylammonium salts **9–13** have been synthesised and tested in nine cancer (MDA-MB-231, MCF-7, HeLa, HepG2, SKBR-3, SKOV-3, PC-3, U-87, and A-549) and two normal (CCD39Lu and HDF) cell lines. The biological activities of these compounds were compared with those of **GDM** and C(17)-analogues **1–7**. Structural studies of **1–13** using 1D and 2D NMR and x-ray crystallography methods revealed nearly identical conformation of the *ansa*-bridge, the *trans* configuration of the lactam group and similar arrangement of the C(17) substituents relative to the quinone core in solution and in solid. The MTT assay revealed that **8** is the most active derivative among studied C(17)-analogues of **GDM** in the 1st panel of MDA-MB-231, MCF-7, HeLa and HepG2 cancer cell lines at low  $IC_{50s} \sim 0.1–1$   $\mu$ M. The anticancer activities of **8** in these cancer cell lines were markedly higher than **GDM**, except for the HepG2 cell line. A higher potency of **8** than **GDM** was noted also in the A-549 cell line of the 2nd panel. Unfortunately, alongside the attractive potency of **8**, higher and lower toxicities than **GDM** were noted in CCD39Lu and HDF normal cell lines, respectively. Studies in MCF-7 cancer cell line revealed improved activities of *N*-alkylammonium salts **9–13** when compared to **GDM** (e.g.  $IC_{50(13)} = 2.31$   $\mu$ M vs.  $IC_{50(GDM)} = 3.51$   $\mu$ M), at together reduced toxic effects in HDF and CCD39Lu normal cell lines ( $IC_{50}$  even  $> 10$   $\mu$ M). Our studies showed that the limited toxicity of **9–13** salts can be linked with their low *clogP* and improved water solubility relative to **GDM** (almost water-insoluble). In studied cancer cell lines, among **9–13** salts the most potent were those without heteroatoms in the attached tail at the nitrogen of C(17)-quinuclidine basket. Molecular docking of the most potent salts **8**, **10**, and **13** indicated the intermolecular hydrophobic stabilisation of the quaternary C(17)-quinuclidine arm with K58 or with Y61 of Hsp90. A more beneficial binding energy of the **8**-Hsp90 complex than that for **10** or **13** complexes explains a higher anticancer activity of **8** than **10** and **13**. Our studies also showed that quaternisation of the nitrogen within C(17)-quinuclidine containing arm can be a useful strategy in decreasing the toxicity of **GDM** analogues in normal cells, at a simultaneously improved or preserved anticancer activity in MCF-7 and A-549 cancer cell lines, respectively (e.g. compound **10**). The use of **13** with potentiator **PEI** leads to improved or comparable anticancer activities relative to those of the salt and **PEI**, respectively. However, this beneficial anticancer



effect was observed at the expense of increased toxicity in normal cells, when referred to **13**.

### Disclosure statement

No potential conflict of interest was reported by the author(s).

### Funding

This work was supported by the Polish National Science Centre (NCN) under Grant Opus 13 no. UMO-2017/25/B/ST5/00291.

### References

- Baksh A, Kepplinger B, Isah HA, et al. Production of 17-O-demethyl-geldanamycin, a cytotoxic ansamycin polyketide, by streptomyces hygroscopicus DEM20745. *Nat Prod Res* 2017;31:1895–900.
- Franke J, Eichner S, Zeilinger C, Kirschning A. Targeting heat-shock-protein 90 (Hsp90) by natural products: geldanamycin, a show case in cancer therapy. *Nat Prod Rep* 2013; 30:1299–323.
- Fukuyo Y, Hunt CR, Horikoshi N. Geldanamycin and its anti-cancer activities. *Cancer Lett* 2010;290:24–35.
- Hermane J, Eichner S, Mancuso L, et al. New geldanamycin derivatives with anti Hsp properties by mutasynthesis. *Org Biomol Chem* 2019;17:5269–78.
- Guo W, Reigan P, Siegel D, Ross D. Enzymatic reduction and glutathione conjugation of benzoquinone ansamycin heat shock protein 90 inhibitors: relevance for toxicity and mechanism of action. *Drug Metab Dispos* 2008;36:2050–7.
- Cysyk RL, Parker RJ, Barchi JJ, et al. Reaction of geldanamycin and C17-substituted analogues with glutathione: product identifications and pharmacological implications. *Chem Res Toxicol* 2006;19:376–81.
- Skrzypczak N, Pyta K, Ruszkowski P, et al. Synthesis, structure and anticancer activity of new geldanamycin amine analogs containing C(17)- or C(20)- flexible and rigid arms as well as closed or open ansa-bridges. *Eur J Med Chem* 2020; 202:112624.
- Kitson RRA, Moody CJ. An improved route to 19-substituted geldanamycins as novel Hsp90 inhibitors-potential therapeutics in cancer and neurodegeneration. *Chem Commun (Camb)* 2013;49:8441–3.
- Li Z, Jia L, Wang J, et al. Discovery of diamine-linked 17-aroylamido-17-demethoxygeldanamycins as potent Hsp90 inhibitors. *Eur J Med Chem* 2014;87:346–63.
- Eichner S, Eichner T, Floss HG, et al. Broad substrate specificity of the amide synthase in *S. hygroscopicus*-new 20-membered macrolactones derived from geldanamycin. *J Am Chem Soc* 2012;134:1673–9.
- Mellatyar H, Talaei S, Pilehvar-Soltanahmadi Y, et al. Targeted cancer therapy through 17-DMAG as an Hsp90 inhibitor: overview and current State of the art. *Biomed Pharmacother* 2018;102:608–17.
- Talaei S, Mellatyar H, Asadi A, et al. Spotlight on 17-AAG as an Hsp90 inhibitor for molecular targeted cancer treatment. *Chem Biol Drug Design* 2019;93:760–86.
- Glaze ER, Lambert AL, Smith AC, et al. Preclinical toxicity of a geldanamycin analog, 17-(dimethylaminoethylamino)-17-demethoxygeldanamycin (17-DMAG), in rats and dogs: potential clinical relevance. *Cancer Chemother Pharmacol* 2005;56:637–47.
- Wu CZ, Jang JH, Woo M, et al. Enzymatic glycosylation of nonbenzoquinone geldanamycin analogs via bacillus UDP-glycosyltransferase. *Appl Environ Microbiol* 2012;78:7680–6.
- Hermane J, Bułyszko I, Eichner S, et al. New, non-Quinone fluorogeldanamycin derivatives strongly inhibit Hsp90. *ChemBioChem* 2015;16:302–11.
- Mohammadi-Ostad-Kalayeh S, Stahl F, Scheper T, et al. Heat shock proteins revisited: using a mutasynthetically generated reblastatin library to compare the inhibition of human and *Leishmania* Hsp90s. *ChemBioChem* 2018;19:562–74.
- Kirschning A, Hahn F. Merging chemical synthesis and biosynthesis: a new chapter in the total synthesis of natural products and natural product libraries. *Angew Chem Int Ed Engl* 2012;51:4012–22.
- Bułyszko I, Dräger G, Klänge A, Kirschning A. Evaluation of the synthetic potential of an AHBA knockout mutant of the rifamycin producer *Amycolatopsis Mediterranei*. *Chemistry* 2015;21:19231–42.
- Eichner S, Knobloch T, Floss HG, et al. The interplay between mutasynthesis and semisynthesis: generation and evaluation of an ansamitocin library. *Angew Chem Int Ed Engl* 2012;51: 752–7.
- Mancuso L, Jürjens G, Hermane J, et al. Bioreduction of aryl azides during mutasynthesis of new ansamitocins. *Org Lett* 2013;15:4442–5.
- Harmrolfs K, Mancuso L, Drung B, et al. Preparation of New Alkyne-Modified Ansamitocins by Mutasynthesis. *Beilstein J Org Chem* 2014;10:535–43.
- Schax E, Walter JG, Märzhäuser H, et al. Microarray-based screening of heat shock protein inhibitors. *J Biotechnol* 2014;180:1–9.
- Tian ZQ, Liu Y, Zhang D, et al. Synthesis and biological activities of novel 17-aminogeldanamycin derivatives. *Bioorg Med Chem* 2004;12:5317–29.
- Greish K, Ray A, Bauer H, et al. Anticancer and antiangiogenic activity of HPMA copolymer-aminohexylgeldanamycin-RGDfK conjugates for prostate cancer therapy. *J Control Release* 2011;151:263–70.
- Li L, Wang L, You QD, Xu XL. Heat shock protein 90 inhibitors: an update on achievements, challenges, and future directions. *J Med Chem* 2020;63:1798–822.
- Raman S, Singh M, Tatu U, Suguna K. First structural view of a peptide interacting with the nucleotide binding domain of heat shock protein 90. *Sci Rep* 2015;5:17015–0.
- Stebbins CE, Russo AA, Schneider C, et al. Crystal structure of an Hsp90-geldanamycin complex: targeting of a protein chaperone by an antitumor agent. *Cell* 1997;89:239–50.
- Jez JM, Chen JCH, Rastelli G, et al. Crystal structure and molecular modeling of 17-DMAG in complex with human Hsp90. *Chem Biol* 2003;10:361–8.
- Rastelli G, Tian ZQ, Wang Z, et al. Structure-based design of 7-carbamate analogs of geldanamycin. *Bioorg Med Chem Lett* 2005;15:5016–21.
- Immormino RM, Metzger LE, Reardon PN, et al. Different poses for ligand and chaperone in inhibitor-bound Hsp90 and GRP94: implications for paralog-specific drug design. *J Mol Biol* 2009;388:1033–42.
- Sawarkar R, Roy N, Rao S, et al. Heat shock protein 90 regulates development in dictyostelium discoideum. *J Mol Biol* 2008;383:24–35.

32. Zhang MQ, Gaisser S, Nur-E-Alam M, et al. Optimizing natural products by biosynthetic engineering: discovery of non-quinone Hsp90 inhibitors<sup>†</sup>. *J Med Chem* 2008;51:5494–7.
33. Wernimont AK, Tempel W, Lin YH, et al. Crystal structure of the amino-terminal domain of HSP90 from leishmania major, LMJF33.0312:M1-K213 in the presence of 17-DMAP-geldanamycin. Available from: <https://doi.org/10.2210/pdb3q5j/pdb>
34. Bhat R, Tummalapalli SR, Rotella DP. Progress in the discovery and development of heat shock protein 90 (Hsp90) inhibitors. *J Med Chem* 2014;57:8718–28.
35. Massey AJ. ATPases as drug targets: insights from heat shock proteins 70 and 90. *J Med Chem* 2010;53:7280–6.
36. Kitson RRA, Moody CJ. Learning from nature: advances in geldanamycin- and radicicol-based inhibitors of Hsp90. *J Org Chem* 2013;78:5117–41.
37. Shan G, Peng Z, Li Y, et al. A novel class of geldanamycin derivatives as HCV replication inhibitors targeting on Hsp90: synthesis, structure-activity relationships and anti-HCV activity in GS4.3 replicon cells. *J Antibiot (Tokyo)* 2011;64:177–82.
38. Li YP, Shan GZ, Peng ZG, et al. Synthesis and biological evaluation of heat-shock protein 90 inhibitors: geldanamycin derivatives with broad antiviral activities. *Antivir Chem Chemother* 2010;20:259–68.
39. Anderson I, Low JS, Weston S, et al. Heat shock protein 90 controls HIV-1 reactivation from latency. *Proc Natl Acad Sci USA* 2014;111:E1528–E1537.
40. Schnur RC, Corman ML, Gallaschun RJ, et al. Inhibition of the oncogene product P185erbB-2 in vitro and in vivo by geldanamycin and dihydrogeldanamycin derivatives. *J Med Chem* 1995;38:3806–12.
41. Ge J, Normant E, Porter JR, et al. Design, synthesis, and biological evaluation of hydroquinone derivatives of 17-amino-17-demethoxygeldanamycin as potent, water-soluble inhibitors of Hsp90. *J Med Chem* 2006;49:4606–15.
42. Molinspiration V2018.10. Available from: <https://www.Molinspiration.Com/>
43. Bank, RPD. RCSB PDB - 3Q5J: crystal structure of the amino-terminal domain of HSP90 from Leishmania major, LMJF33.0312: M1-K213 in the presence of 17-DMAP-geldanamycin Available from: <https://www.rcsb.org/structure/3Q5J> [accessed 7 May 2020].
44. Thepchatrri P, Eliseo T, Cicero DO, et al. Relationship among ligand conformations in solution, in the solid state, and at the Hsp90 binding site: geldanamycin and radicicol. *J Am Chem Soc* 2007;129:3127–34.
45. Lee YS, Marcu MG, Neckers L. Quantum chemical calculations and mutational analysis suggest heat shock protein 90 catalyzes trans-cis isomerization of Geldanamycin. *Chem Biol* 2004;11:991–8.
46. Scigress package FJ 2.6/EU 3.1.9./2008–2019; Japan: Fujitsu.
47. Douafer H, Andrieu V, Phanstiel O, Brunel JM. Antibiotic adjuvants: make antibiotics great again!. *J Med Chem* 2019; 62:8665–81.
48. Liu TY, Hussein WM, Giddam AK, et al. Polyacrylate-based delivery system for self-adjuvanting anticancer peptide vaccine. *J Med Chem* 2015;58:888–96.
49. Domalaon R, Idowu T, Zhanel GG, Schweizer F. Antibiotic hybrids: the next generation of agents and adjuvants against gram-negative pathogens? *Clin Microbiol Rev* 2018; 31:e00077–17.